2.1Introduction

The semi-solid processing of alloys has attracted the research interest for several years. Several processing techniques are currently available for effective distribution of liquid phase in its primary solid solution matrix. The solidification behavior of such liquids have been reported in the past by several investigators [Kimet al.1992, Kimandet al.1991, Cantoret al.1979, Southinet al.1978, Kimet al.1991, Chuet al.1984, Ojhaet al.2001, Pandeyet al.1995, Pandeyet al.1994, Ojhaet al.1997 and Pandeyet al.1992]. Southin and Chadwick [Southinet al.1978] investigated undercooling behaviour of liquid present in solid matrix of a large number of binary alloys. Their experimental technique consisted of annealing a hypoeutectic alloy in a semi-solid phase followed by their slow cooling below the eutectic temperature. A thermal peak corresponding to evolution of latent heat of fusion detected in inverse rate cooling curve was taken as the average nucleation temperature. The liquid present along the grain boundary as continuous network exhibited low undercooling in contrast to large undercooling associated with freezing with liquid present in the isolated regions of the matrix. A non-reciprocal nucleation behaviour of the primary solid phases was observed to be the characteristic features of the alloys. As per their observation if α- phase is good nucleant for β phase, then the β phase was observed to be a poor nucleant for the α-phase. Their result was further analysed by [Cantoret al.1979] to predict the nucleation temperature of the melt. These investigators in their analysis considered nucleation of an equilibrium phase. However, later on investigation of Ojha et al. [Ojhaet al.2001, Pandeyet al.1995, Pandeyet al.1994 and Ojhaet al.1997] revealed that in such experiments a metastable phase nucleates referentially over a stable phase at large undercooling of the liquid entrained in the matrix of its primary phase. Formation of two metastable phases with rhombohedral and monoclinic crystal structure was reported in Al-Ge alloys. The scale of the liquid

droplets was considerably reduced in alloys subjected to rapid solidification [Ramachandraraoet al.1979]. These investigations indicated interesting orientation relationship between the matrix and second phase particles.Although these provided a valuable insight into solidification behaviour of droplets entrained in their primary solid phases but the mechanical and tribological characteristics of such composite structure have not been studied. The present investigation constitutes an attempt in this direction. Al-10Cu alloy has been selected for the study. This is a long freezing range alloy suitable for semi-solid processing. The alloy possesses high strength and wear resistance and this is attractive for use in aircraft cylinder heads and in automotives as pistons and cylinder blocks. Their freezing characteristics and tribological behaviour are reported.

2.2 Experimental details

2.2.1 Preparation of Al-10Cu alloy

The Al-10Cu alloy was prepared in a graphite crucible using electric resistance heating furnace. A superheating of 200 K was consistently maintained. The melt was stirred to ensure melt homogeneity. The melt was poured into a rectangular cross section cast iron mould after degassing with the hexachlroethane. A typical composition of the alloy is shown in Table (1). The samples were cut into 20mm x 20mm x 12mm sizes for microscopic and hardness studies and 50mmx50mmx12mm for wear testing. Cylindrical samples of 10 mm diameter and 10 mm length were machined for undercooling experiments.

Table1: Chemical composition of Al-10Cualloy.

Element	Si	Fe	Cu	Mn	Mg	Zn	Pb	Sn	Al
Weight %	0.686	0.615	10	0.326	0.082	0.655	0.0190	0.0257	Bal.

2.2.2 Thermal cycling of as cast alloy

For thermal cycling of the alloy vertical resistance heating furnace was used. The cylindrical sample was place in a silica crucible. The sample was drilled for a fine hole to insert one end of the chromel-alumel thermocouple with other end connected to highly sensitive micro-voltmeter. The sample was slowly heated to 560°C i.e. 12°C above the eutectic temperature of the alloy as shown in Fig.2.1. After holding for 30 minutes the sample was cooled to a temperature below the eutectic temperature.

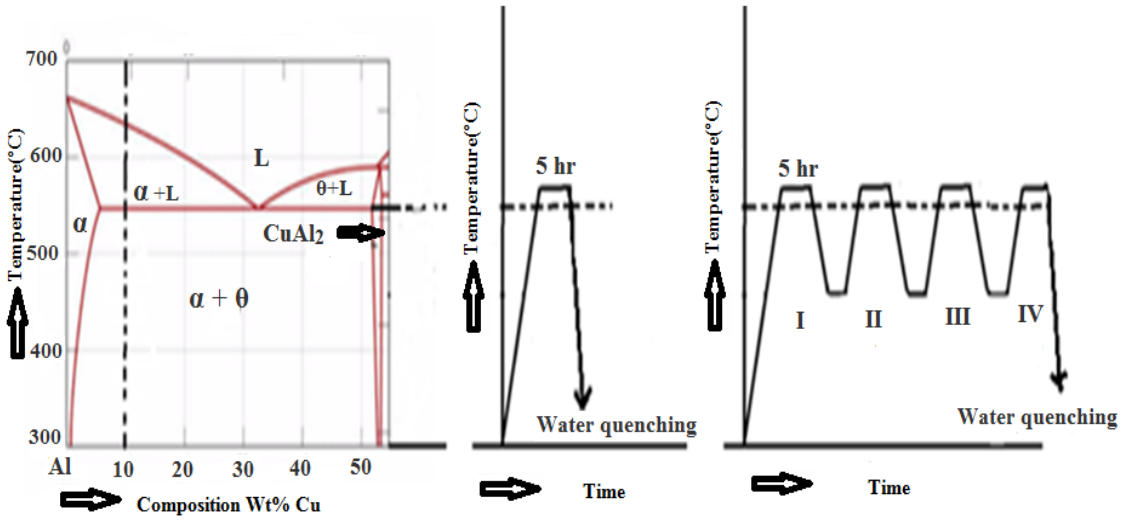

Figure 2.1: Schematic diagram showing thermal cycles of the alloy from 560 °C from different hold time (a) single cycle for 5hrs (b) four cycles for 5hr holding time.

The above thermal cycle was consequently repeated four times before the sample was quenched in water. The temperature was recorded during the cooling cycle for each 5°C drop in temperature through chromel-alumel thermocouple. The nucleation temperature of the melt was indicated by the peaks generated through the inverse rate cooling curve plot.

The samples were heated to 560°C and held for 5hrs and quenched in water and other sample was left in the furnace to repeat the thermal cycling for several times. At the end of the fourth cycle towards the end of approximately 5hrs annealing time, specimen was quenched in water.

2.2.3 Microstructural examination

Samples for microstructural examination were extracted from Al-10Cu alloy and were prepared following standard metallographic techniques. Keller's reagent (1% vol. HF, 1.5% vol. HCl, 2.5% vol. HNO_3 and balance water) was used for etching the polished samples. Leica Optical Metallograph attached to image analyser was used to examine the microstructure of the samples. SEM (FESEM Quanta 200FEG) was used to study the morphology of the alloy and EDS (Model-51-ADD0048) was used to analyse the debris on wear track.Before doing the hardness test all the samples were polished and cleaned with the acetone. LECOLV700AT Vickers hardness tester was used at a load of 5kg for the hardness study. For each sample minimum five measurements were taken for getting the average value of hardness. The hardness of the matrix as well as that of droplet solidified areas were examined using a Tukonmicrohardness tester at a load of 50g.

2.2.4 Wear testing

DUCOM TR-20 pin-on-disc machine (Bangalore, India) was used to carry out the sliding wear test of the cast alloy. A cylindrical specimen with 8mm diameter and 30mm length was held against EN31 steel disc 60 HRC. Ultrasonic cleaner with acetone was used to clean the sample and weighed to an accuracy of ±0.1mg before testing at every 10 min intervals. At room temperature only wear test was carried out and the test was repeated three times for each and individual load to avoid errors. The wear testing was conducted at different loads ranging from 10-50N at a sliding speed of 1.0m/s and a

sliding distance of 3000m. Volumetric loss was calculated by weight loss and density measurement using Archimedes' principle. During the test the value of friction was monitored using a load cell attached to the setup. For evaluating the wear rate at different loads standard wear procedure was followed.

2.3. Results and discussion

2.3.1 Undercooling behaviour

Figure 2.2shows results of thermal cycling. There is a distinct peak observed at a temperature 530°C.This amounts to an undercooling of 16°C below the eutectic. Besides, several smaller peaks are observed between 520to 500°C. This corresponds to nucleation temperature of different isolated droplets. Once the average temperature of nucleation is taken to be 510°C. This amounts to an undercooling of 36°C below eutectic temperature for nucleation of droplets. The quantitative metallographic measurements indicated that the droplet sizes range from 10-50 μm under the experimental conditions employed. In the present study indicates that the undercooling of the melt increases with thermal cycling of the sample. This observation is supported with the work of Pandey and Ojha [Pandey and Ojha, 1997]. When the alloy is heated above its eutectic temperature during its initial stages of homogenization. The interdendritic phase melts and forms a continuous network. When the same alloy is subjected to slow cooling the sample provides low undercooling of liquid. When the alloy is subjected to this type of repeated thermal cycling for long soaking time for equilibrium it generates isolated droplets entrained in the primary phase. At the initial stages of homogenization the continuous liquid network will form along the grain boundaries. The whole liquid can freeze with even one nucleation event. The isolated droplets are nucleated independently and so they may nucleate at larger undercooling of the melt [Southin and Chadwick, 1978]. Thermal cycling changes the potency of the nucleant in the melt [Ojhaet al.1983 and Ojhaet

al.1982]. Ojha et al. [Ojha, 1991] explained importance of undercooling behaviour of droplets entrained in the solid phase. The as cast alloy held in the furnace at 560°C for 5hrs has initially shown a continuous network of liquid phase. During thermal cycling this liquid network breaks into irregular small liquid networks distributed randomly. At the fourth cycle optical microstructure indicates the breaking of the continuous network leading to formation of small liquid droplets.

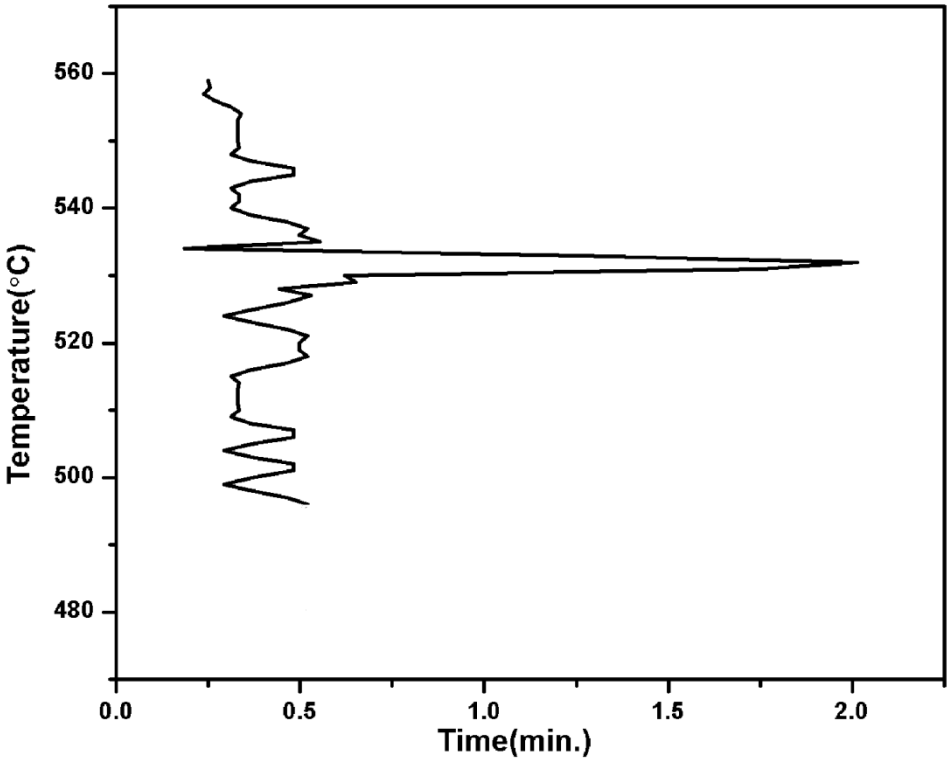

Figure 2.2: Typical inverse rate cooling curve of Al-10Cu alloy.

2.3.2 Microstructural features

A hypo-eutectic alloy based on Al-Cu system was thermally cycled between semi-solid regions to low temperatures. Fig. 2.3(a) shows the microstructure of the as cast alloy indicates e dendritic structure. Fig. 2.3(b) shows continuous network around the primary grains of the α –aluminum phase resulted from the melting of eutectic phases in the interdendritic region when the alloy is subjected to thermal cycling. Fig.2.3(c) shows

wide range of liquid droplets distributed in the solid matrix as well as entrained in the grains. This is due to the intergranular eutectic phase which was subjected to repeated melting and cooling from the semi-solid region to below the eutectic temperature leads this droplet formation. The larger size droplets are surrounded by finer droplets. Larger droplets are the source for forming the finer droplets this is because the region adjacent to the droplets are depleted of solute. This observation was also presented by Pandey and Ojha [Pandey and Ojha, 1997] in undercooling behavior of Ag-Ge alloys. These liquid droplets subjected to larger undercooling compared to continuous liquid network of eutectic along the grain boundaries [Ramachandrarao et al. 1992]. Fig. 2.3(d) shows droplets are entrained in the grains. It is also noted that there is considerable difference in hardness measurement on the primary phase and the droplet of the thermally cycled alloy. The morphology of the primary phase also changed from dendritic to a spherical. This type transition has been observed by several other investigators [Kattamis and Flemings, 1967 and Walder and Ryder, 1993]. The size of the droplets varied from 10 to 200μm arising from migration of liquid under temperature and concentration gradient. The size of the droplets depends upon the number of thermal cycles of the specimen and holding time in the semisolid region for equilibration of the alloy. The SEM examination also reveals the similar feature and EDS analysis provided constitution of droplets regions. The higher magnification observation reveals the more details of the fine droplets. Fig. 2.4(a) shows wide range of liquid droplets distributed in the solid matrix which was held at 560°C i.e. above the eutectic temperature for 5hrs and followed by four thermal cycles. Fig. 2.4(b) indicates the droplets entrained in the grains. The presence of micropores in interdendritic sites [Bala and Lund, 1979] or existence of crystalline defects may be responsible for nucleation of liquid globules inside the grains [Vernhoven and Gibson, 1971].

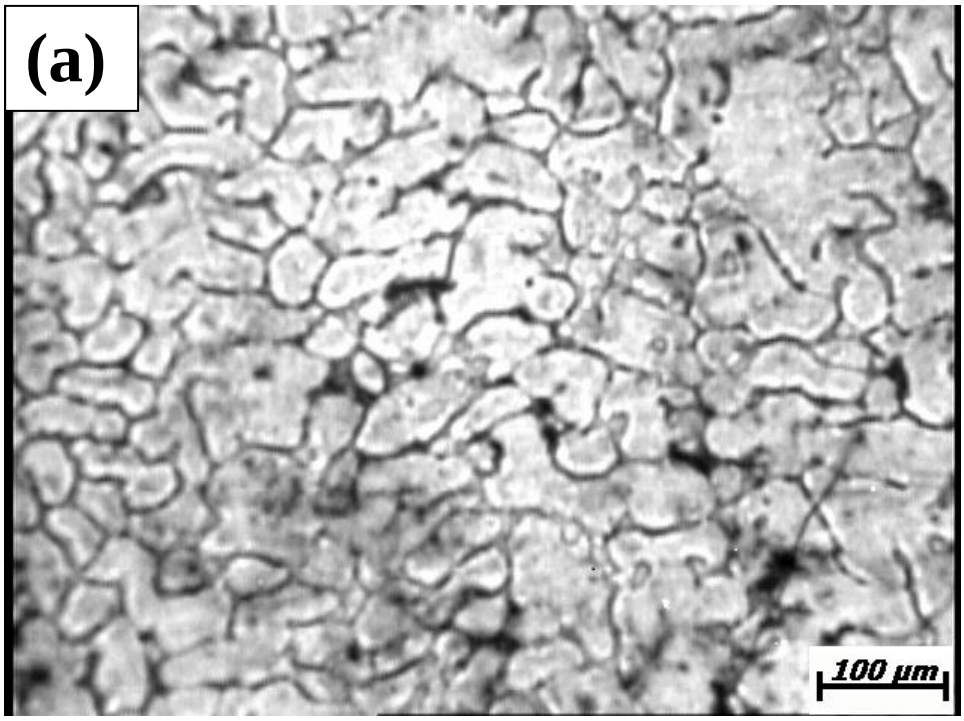
(a)
100 µm

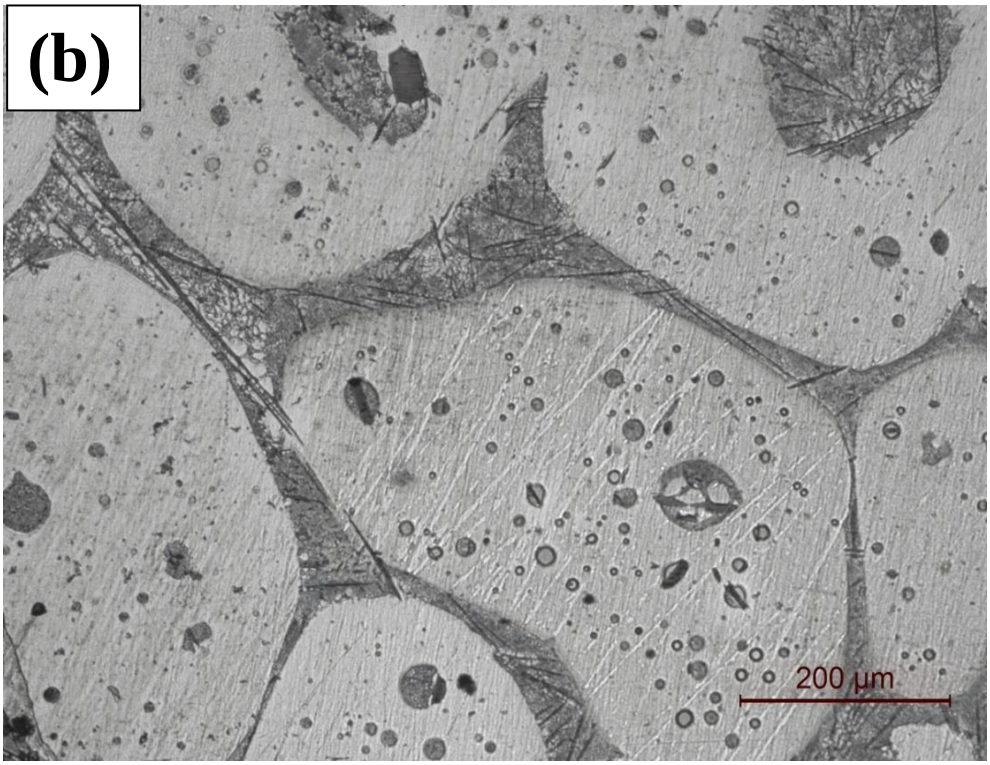
(b)
200 µm

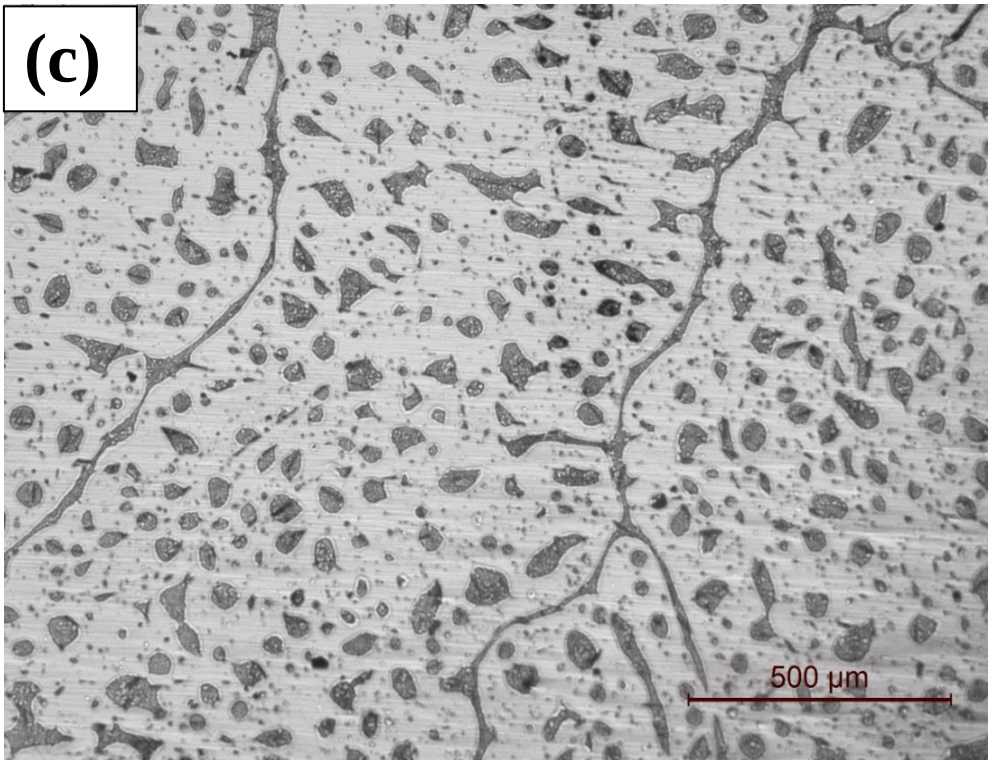

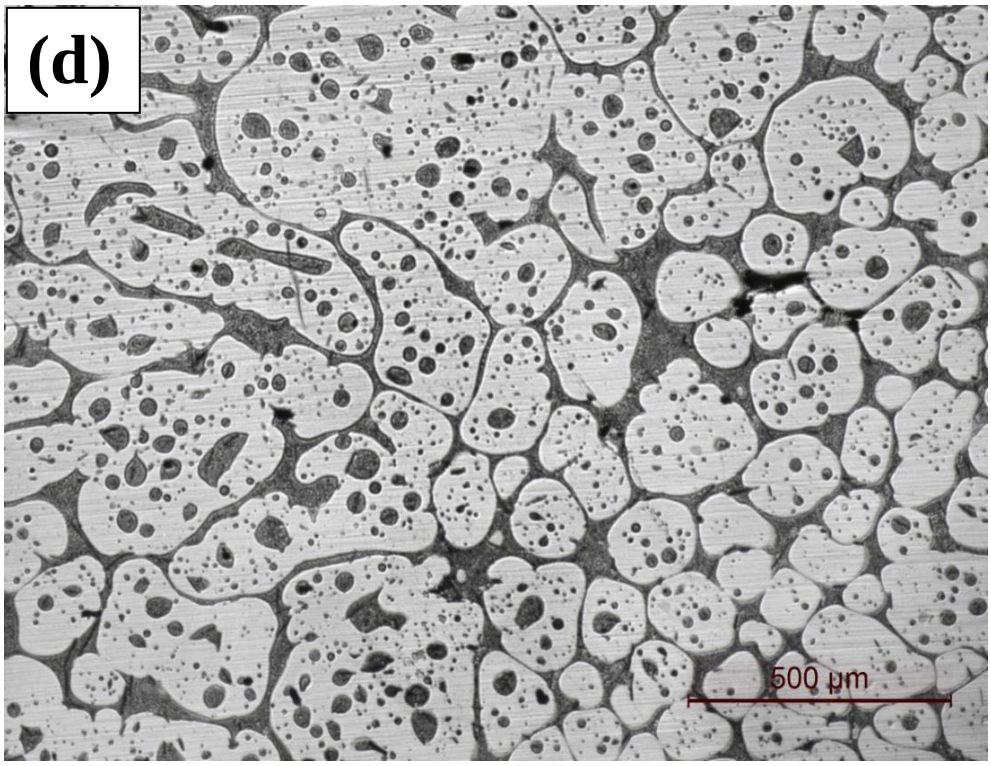

Figure2.3: Optical micrographs of (a) as cast alloy showing dendritic structure and (b) to (d) cast alloy subjected to four thermal cycle from 560 to 300 ^{o}C held for 5hrs showing a progressive change in size and size distribution of liquid phase.

The solidification structure of droplets exhibited presence of fine particulate morphology of the eutectic phases in contrast to coarse lamellar eutectic microstructure in the inter-dendritic region of the as cast alloys. The decomposition of supersaturated solid solution phase resulting from large undercooling of droplets were explained for this anomalous behavior of the eutectic.

The average hardness values of the as cast, the first thermal cycle and four thermal cycled alloys are 90 Hv, 96 Hv and 110 Hv, respectively. The hardness of the matrix as well as that of droplet solidified areas were examined and found 152 Hv for the matrix and 267 Hv for its droplets. The EDS analysis of these droplets reveal that they contain aluminum and copper .The detailed EDS analysis was shown for the droplet and as well for the matrix also in the figure2.5(a) & 2.5(b) droplets were examined in the SEM for more details.

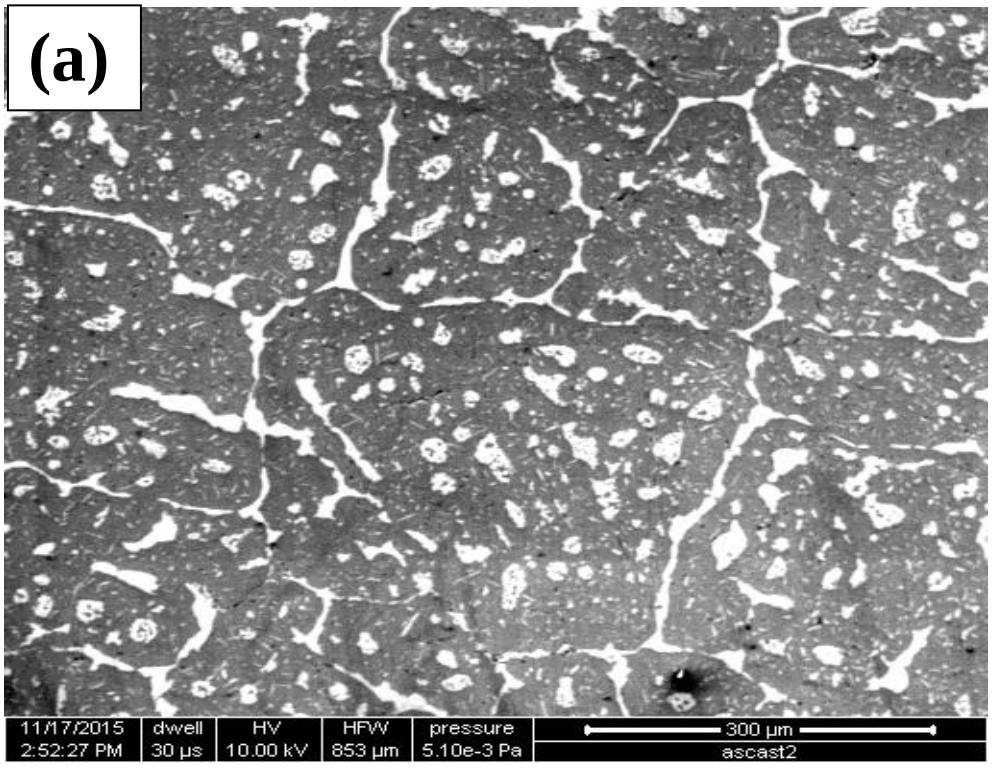

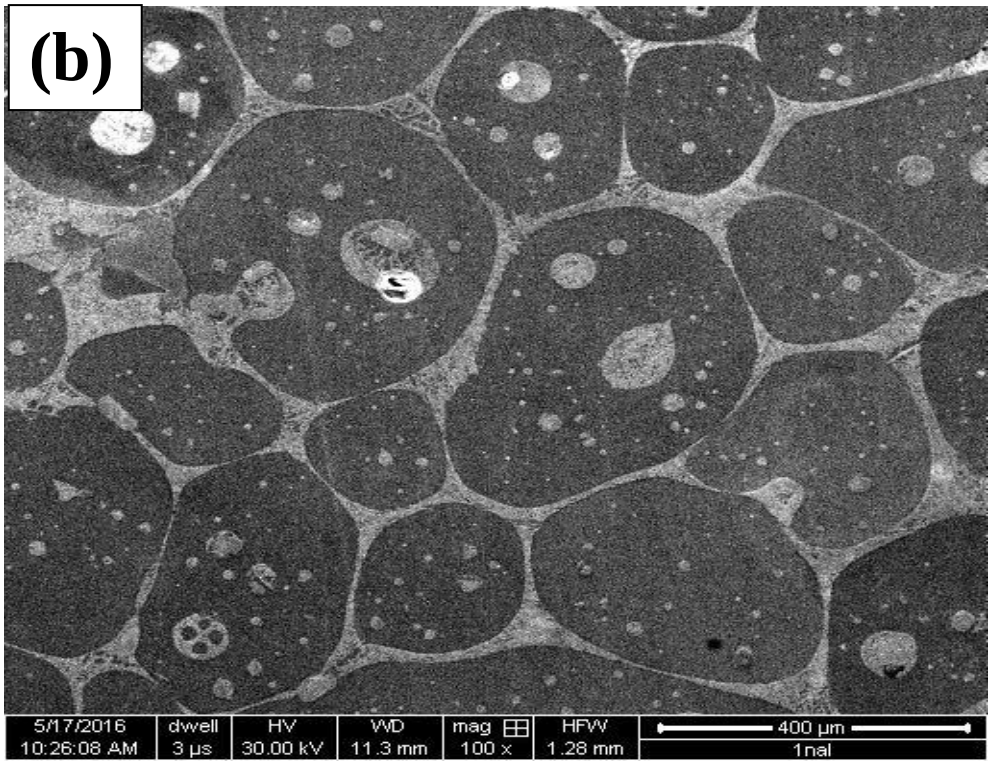

Figure2.4: SEM micrographs of four thermal cycled alloy at 560 °C hold for 5hrs (a) liquid pockets distributed in the matrix (b) liquid droplets entrained in the grains thermal cycle.

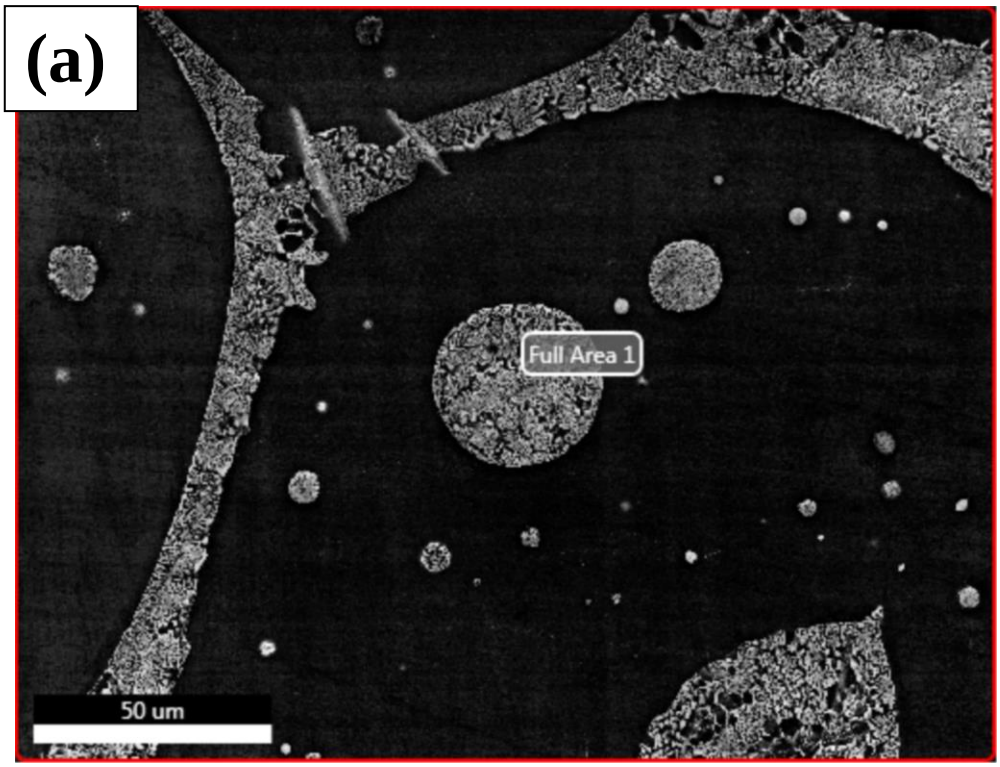

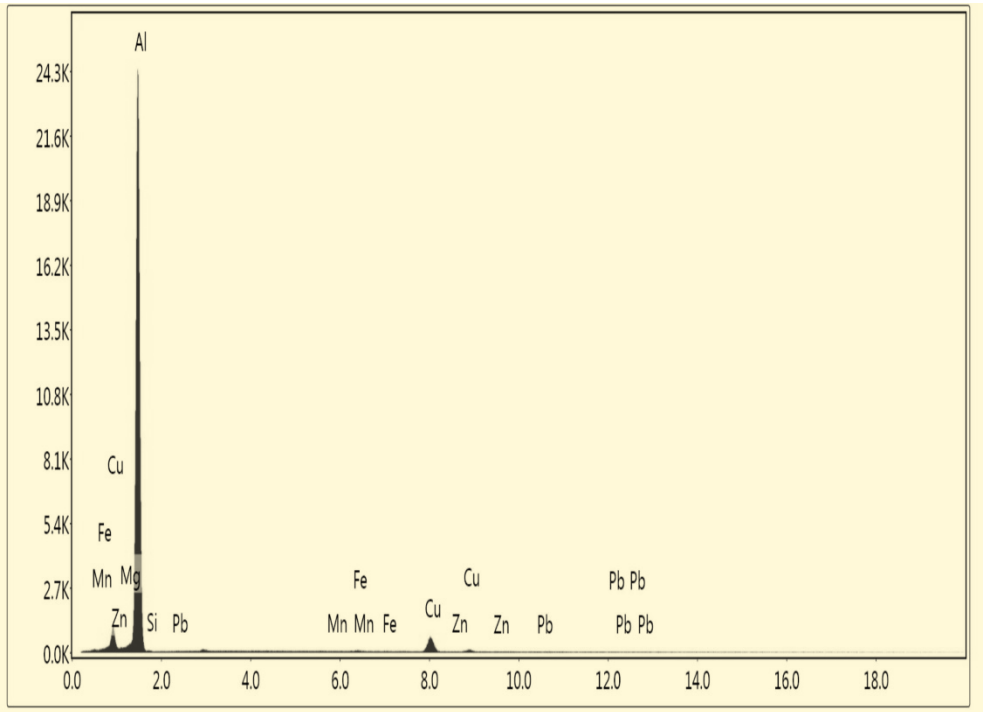
Al
24.3K
21.6K
18.9K
16.2K
13.5K
10.8K
8.1K
5.4K
2.7K
0.0K
Cu
Fe
Mn Mg
Zn
Si
Pb
Fe
Mn Mn Fe
Cu
Cu
Zn
Zn
Pb
Pb Pb
Pb Pb
0.0
2.0
4.0
6.0
8.0
10.0
12.0
14.0
16.0
18.0
Lsec: 17.3 0 Cnts 0.000 keV Det: Element-C2 Det

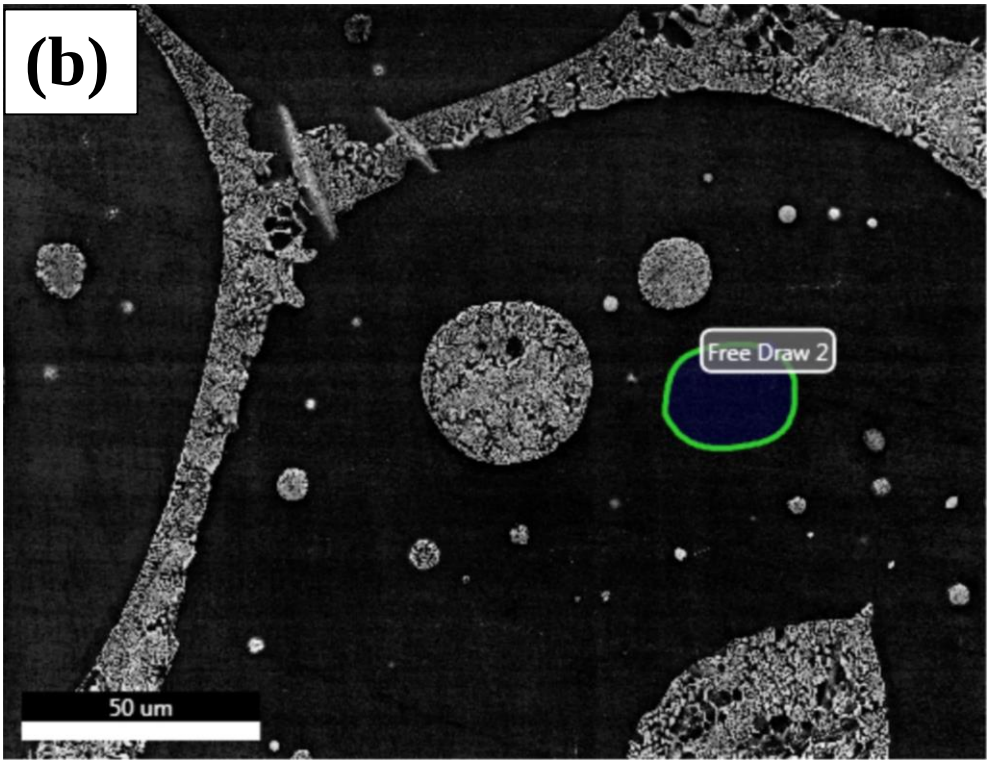
(b)
Free Draw 2
50 um

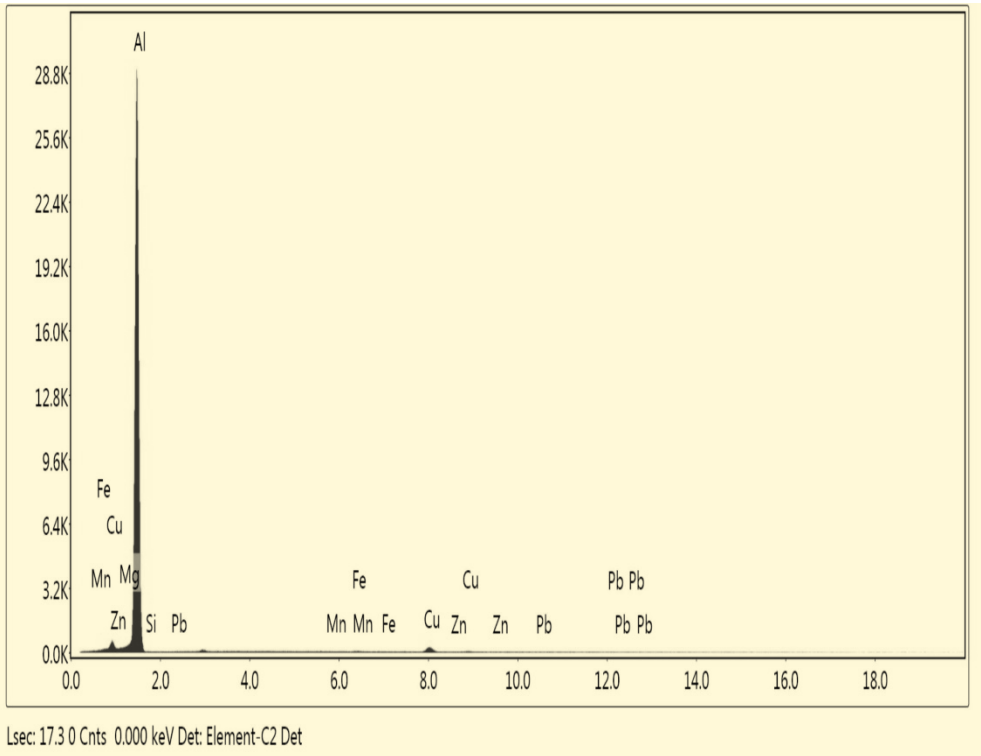

Figure 2.5:(a) EDS analysis of the droplets formed during the 4th thermal cycle of the Al-10Cu alloy, (b) EDS analysis of the solid matrix on which droplets were formed during the 4th thermal cycle.

2.3.3. Wear characteristics of Alloy

The wear characteristics of Al-10Cu-Si alloy in as cast and after thermal cycling condition for a range of applied load 10 to 50N at a sliding distance of 3000m are shown in the Fig.2.6. These represents the variation of the cumulative volume loss of as cast and thermal cycled alloys with the sliding distance at a sliding velocity of 1.0 m/s. In Fig.2.6 (a) at 10N load the volume loss is observed to increase with increase in the sliding distance irrespective of the alloy processing condition. However, thermal cycled alloys show less cumulative volume loss compared to the as cast alloy. The alloy subjected to four thermal cycles indicated less cumulative volume loss compared to as cast and single thermal cycled alloy. The rate of change in cumulative volume loss is also not rapid in case of four thermal cycled alloy compare to the as cast and single thermal cycled alloy.

Fig.2.6 (a) shows that the cumulative volume loss of the as cast alloy increases with increase in sliding distance up to a maximum value of 6.7 mm^3 for the total sliding distance of 3000m. The cumulative volume loss of four thermal cycled alloy is less than that of the as cast alloy. The cumulative volume loss of the 1st thermal cycled alloy is 0.35 mm^3 at a sliding distance of 600m and increased to 2.5mm^3 at 3000m. Fig.2.6 (b) represents that the cumulative volume loss has increased with increase in sliding distance for the as cast and thermal cycled alloys at 20N. The cumulative volume loss of as cast alloy is two times more than that of the as four thermal cycled alloy. Fig.2.6(c) also shows an increasing trend of cumulative volume loss with an increase in sliding distance. This means that the cumulative volume loss of four thermal cycled alloy is 2.3 times less compared to as cast alloy. A similar trend was also observed at higher load of 40 and 50N as shown in Fig.2.6(d & e). The slope of the wear loss graphs provided the information on wear rate of the materials and theses were deduced from the above experimental data.

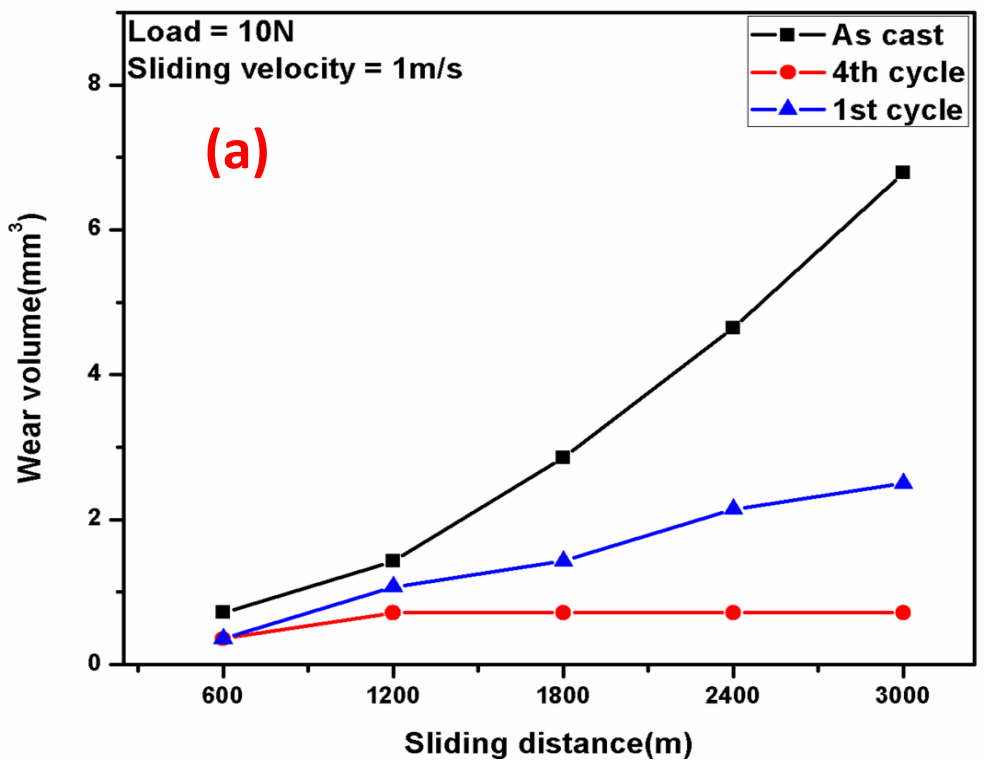

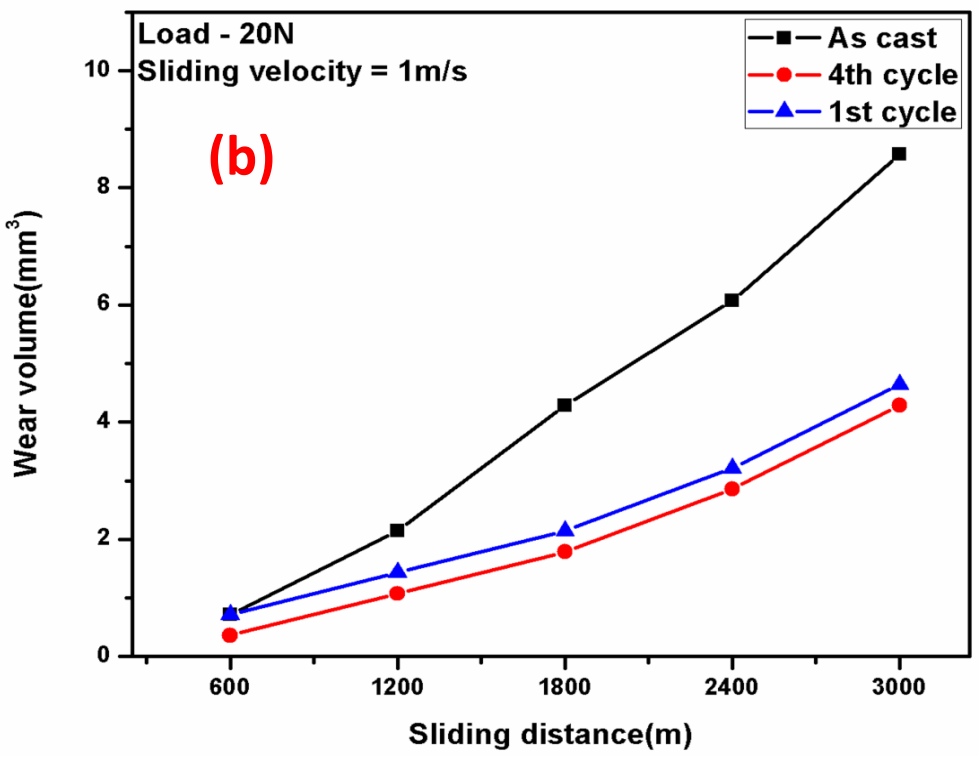
Load - 20N
Sliding velocity = 1m/s
(b)
As cast
4th cycle
1st cycle
Wear volume(mm3)
Sliding distance(m)
0
2
4
6
8
10
600
1200
1800
2400
3000

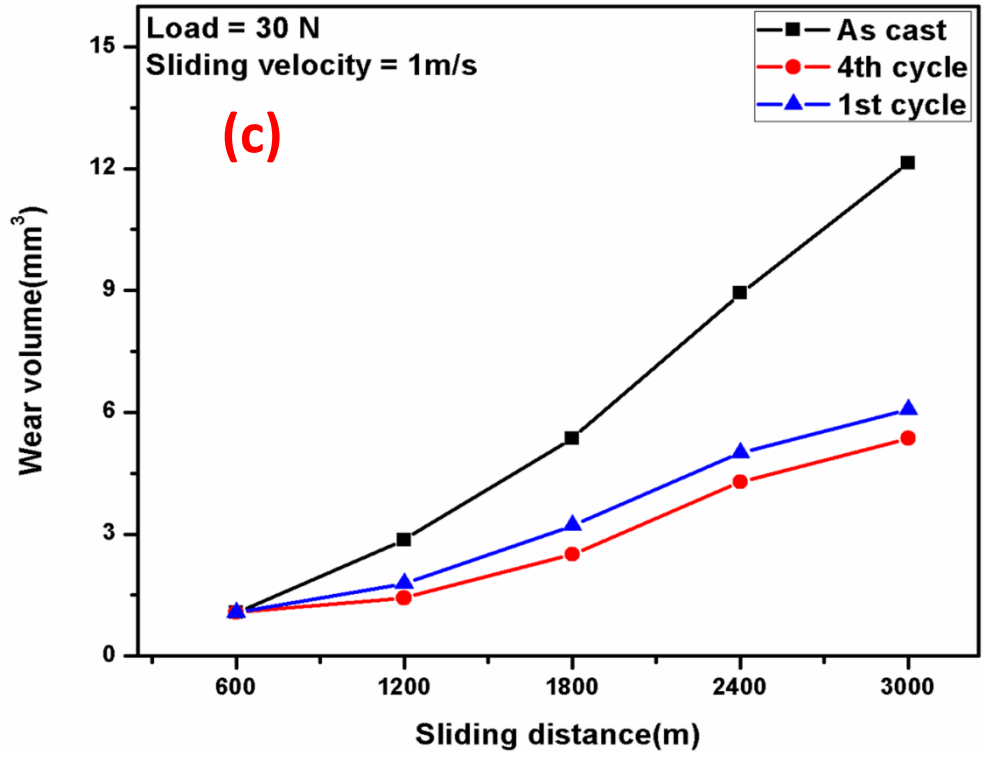
Load = 30 N
Sliding velocity = 1m/s
(c)
As cast
4th cycle
1st cycle
Wear volume(mm3)
Sliding distance(m)
0
3
6
9
12
15
600
1200
1800
2400
3000

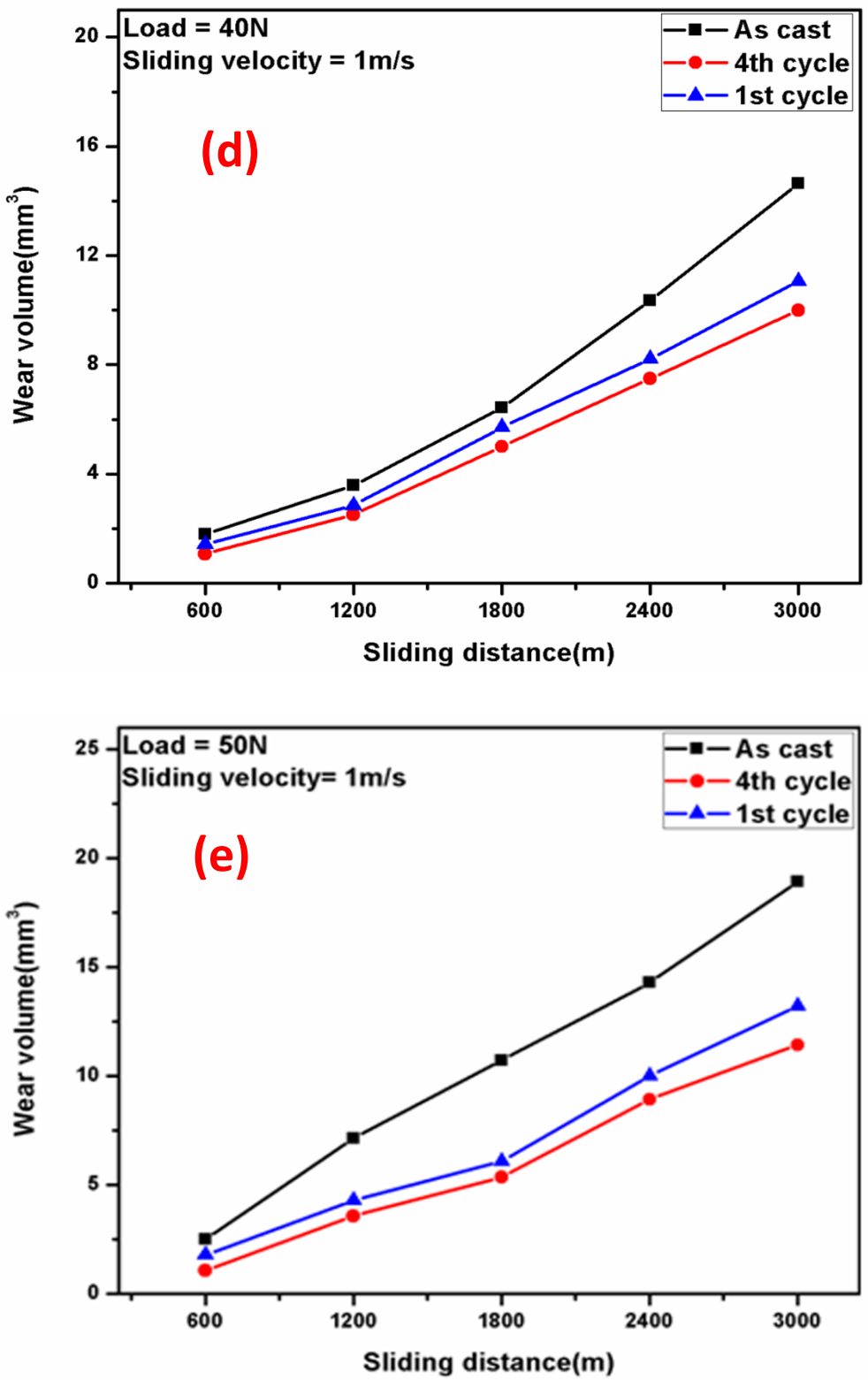

Figure 2.6: Variation of cumulative volume loss with sliding distance (a) at 10N (b) at 20N (c) at 30N (d) at 40N (e) at 50N.

Figure 2.7 shows the variation in the wear rate of the as cast and thermal cycled alloys with applied load. It is clear from the figure that the wear rate of the as cast and as well as the thermal cycled alloy increases with increase in applied load. The wear rate of four thermal cycled alloy is less compared to the as cast and single thermal cycled alloy. The wear rates at the higher load are improved due to thermal cycling. For example, the wear rate of the as cast alloy at an applied load of 10N is considerably lower than that at 50N load.The wear rate of four thermal cycled alloy and single thermal cycled alloys at a load of 50N are observed to be relatively less than that of cast alloys respectively This is indicated by the wear rate of four thermal cycled alloy which is 1.6 times less than that of as cast alloy at 50N load.

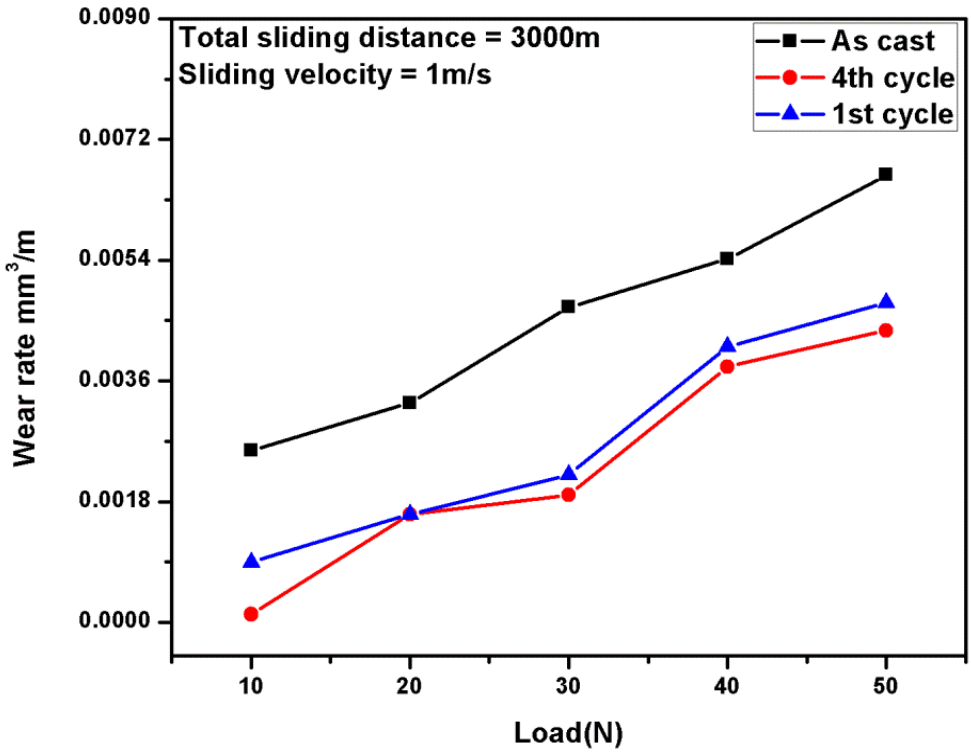

Figure 2.7: Variation of wear rate as a function of normal load of the as cast and thermal cycled alloys.

The coefficient of friction calculated from the frictional force recorded by the system and the applied load on the specimen surface. The coefficient of friction for as cast and its thermal cycled alloys is plotted as a function of sliding distance at a constant sliding velocity of 1.0 m/s and shown in the Fig.2.8 (a). It is observed that the coefficient of friction decreases with increase in load for as cast alloy and other thermal cycled alloys. As cast alloy coefficient of friction is varied from 0.31 to 027. In case of four thermal cycled alloy and first thermal cycled alloy the varied range coefficient of friction is between 0.27 to 0.25 and 0.28 to 0.25. This indicates that the coefficient of friction of the thermal cycled alloy is less at both for 600 and 3000m sliding distances than that of the as cast alloy. The four thermal cycled alloys indicate the maximum decrease in coefficient of friction and minimum wear rate.

The wear rate of as cast and thermal cycled alloys is plotted as a function of applied load at a velocity of 1.0m/s and show in Fig. 2.8 (b). It is noted that the coefficient of friction decreases with increase in load irrespective of alloy processing condition. For example, the wear rate of the as cast alloy at an applied load of 10N is 0.38 and it decreased to 0.26 at an applied load of 50N. In case of four thermal cycled alloy, the coefficient of friction decreased from 0.35 to 0.24 when the applied load is increased to 50N. The higher thermal cycled alloys results in a maximum decrease in coefficient of friction and minimum wear rate.

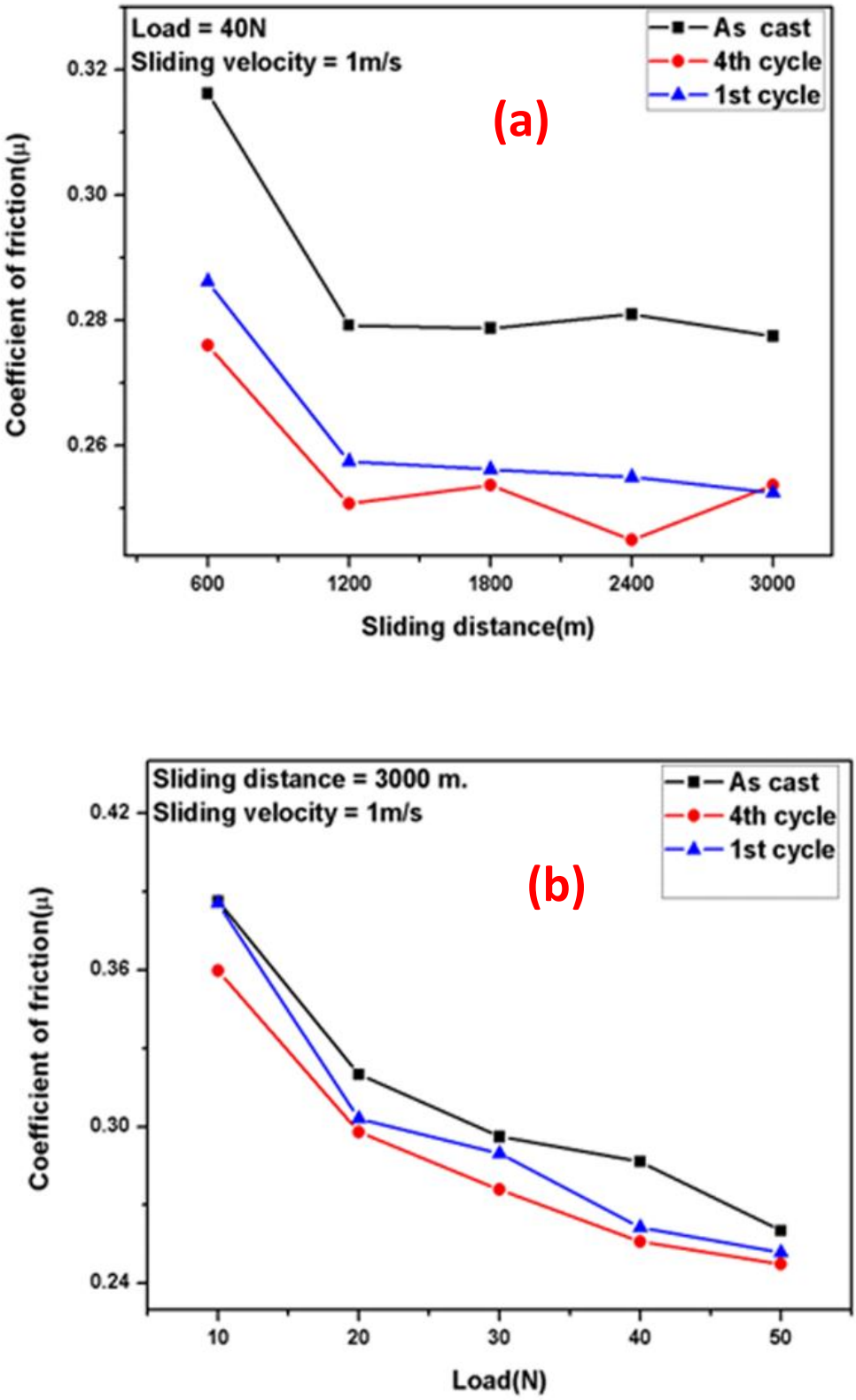

Figure 2.8: Variation of coefficient of friction with (a) sliding distance(b) normal load.

In wear process the real contact between two solid surface is invariably very small when comparing with the apparent area of contact. The contact area continuously changes with the different parameters like type of material in contact, load, sliding distance and sliding velocity. The relative motion causes the progressive loss of material in the form of microcracks or localized deformation [Mandal et al.2009 and Caracostas et al. 1997].In aluminum alloys the surface oxidation is common even at room temperature. The oxide layer generated restricts the metal to metal contact. When normal load increases this oxide layer detaches from the surface due to increase in surface deformation. Deep grooves may be created due to gouging of the surface and the nature of the wear changes from mild to severe. This leads to sharp increase in wear rate.

At low loads micro welds form and grow because more time is available. Force requirement increase to keep the relative motion by shear-off the micro welds. This leads to increase in wear resistance. The wear rate increases with the load because the hard asperities of the counter surfaces cause ploughing and delamination of surface end up with large grooves. With increase in load micro-cracking at subsurface level may happen. During wear run the asperities may be deformed in the subsurface or removed from the surface. At higher loads, the material gets softened and flow stress of the material decreases because of rise in interface temperature and engenders oxidation also. The discrete oxide film formed act as hard impurity or particle between mating surfaces. This may also leads to increase in wear rate [Anasyida and Daud, 2009].

The higher value of coefficient of friction at lower load is shown in the Fig.2.8. This is because of locking of surface asperities where the full surface of the true contact is not established. The SEM micrographs of the worn-out surfaces of thermal cycled Al-10Cu alloy and as cast alloy at load of 30N and 50N are shown in the Fig. 2.9 to 2.11 respectively. Generally dry sliding wear is caused by locking and local welding of surface

asperities and ploughing of the material is due three-body abrasion [Rudrakshi and Ojha, 2007]. The scoring of the as cast worn surfaces is heavier than that of the thermal cycled samples and are extended from one end of the surface to the other end continuously. The as cast alloy exhibited severe wear on the mating surface compared to the thermal cycled alloys at a load of 50N. Adhesion followed by abrasion has proved by the topography of worn-out surfaces. This scoring may be due the hard asperities on the hardened steel disc counterface or entrapped particles caused abrasion or by work-hardened deposits on the counter surface [Dey, Poddar, 2006, Bai and Biswas, 1991, Bai and Biswas, 1983, Reddy et al. 1995 and Wilson and Alpas, 1999]. The worn particle debris are agglomerated and stick to the grooves during wear run. This is because of localized heating generated by friction with increasing load makes the in stick to the disc surface. As pin on the disc slide against each other the increase in interface temperature causes wear debris stick at the grooved surfaces [Doherty et al.1984]. As cast alloys wear rates are higher due to coarse and segregated dendritic microstructures.

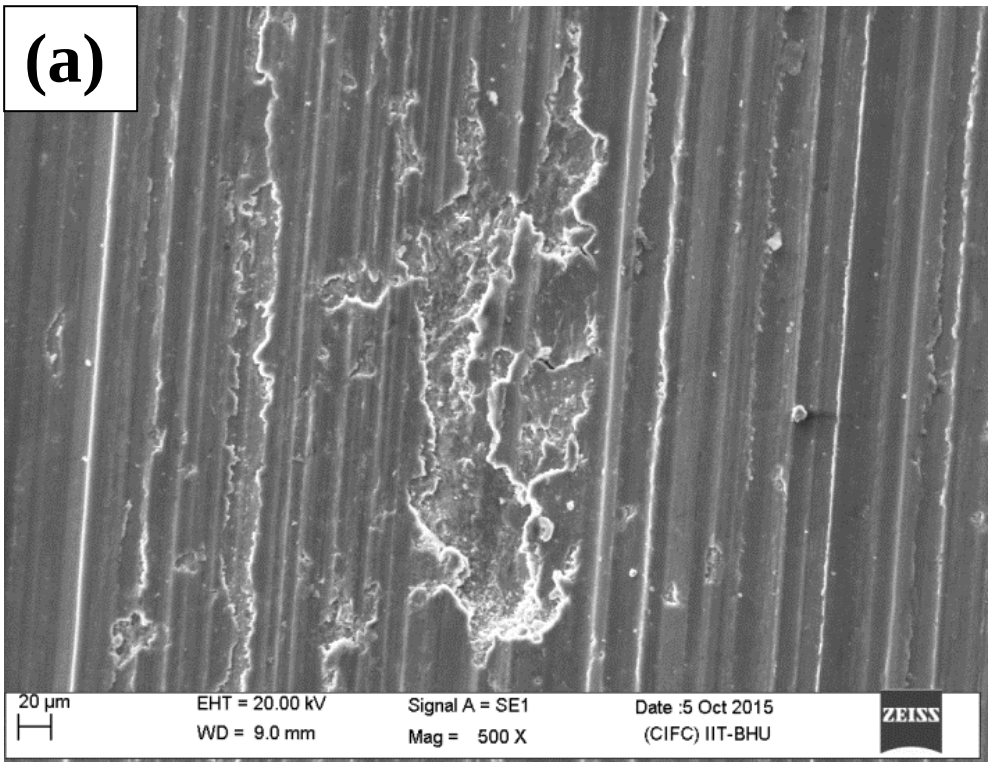

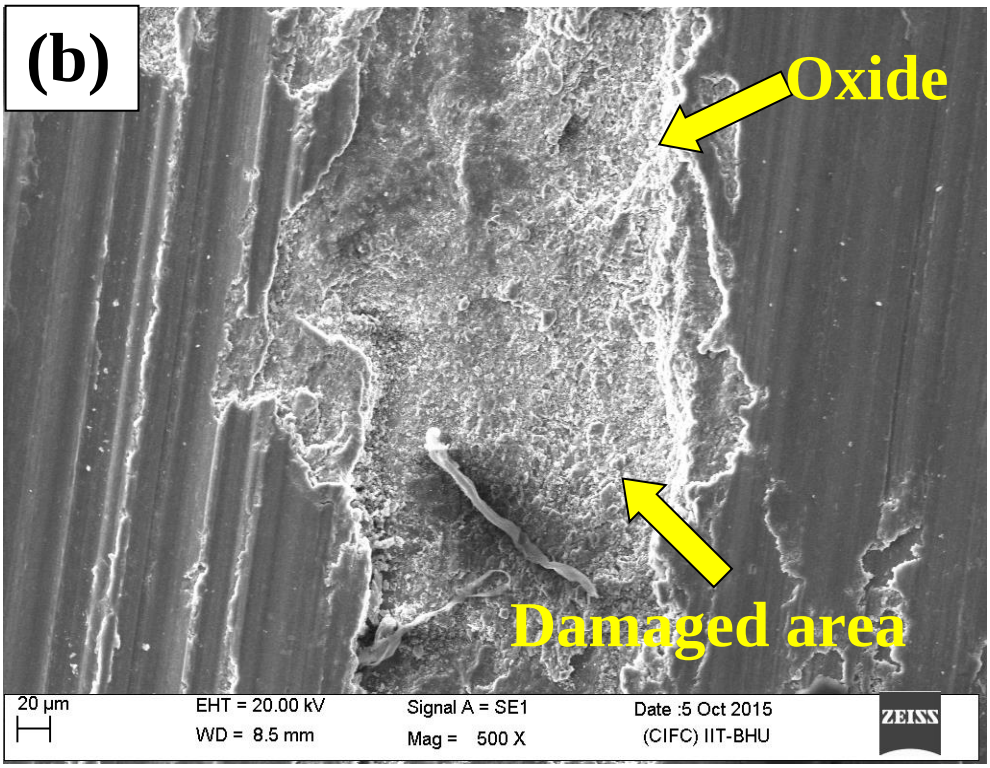

Figure 2.9:SEM micrographs of worn surfaces of the as cast alloy at two different loads (a) 30N (b) 50N showing increasing dimple structure with increase in applied load.

The extensive plastic deformation is indicative of irregular plastic flow lines during wear run. The width of the groove enlarged with increasing the load in case of first therrmal cycled alloy shown in Fig. 2.10. Surfaces are having long continuous grooves which are parallel to the sliding direction. In the sliding direction cracks are propagated. However, the extent of wear in the thermal cycled Al-10Cu alloy samples is lower. Fig. 2.11(a) exhibits large grooves and these are observed in the alloy subjected to metallic wear. Fig. 2.11(b) shows small size grooves with oxide white patches indicating abrasive wear of the sample. The improvement in 4th thermal cycled is due the globular microstructure formed from the as cast dendritic structure [Van et al.2015]. The droplet distribution and their resultant solidification structure resulted in an improvement in tribological characteristics of the alloy. This effect is attributed to the presence of ultrafine solidification structure of droplets arising from their large under cooling. This

feature is evident in the microstructure of droplet regions. In addition, the solute elements are themselves get redistributed differently in droplets vis-a-vis that in the liquid present in the inter-dendritic region of the cast alloy. The EDAX analysis of droplet regions and that of the bulk liquid region provides support in this direction.

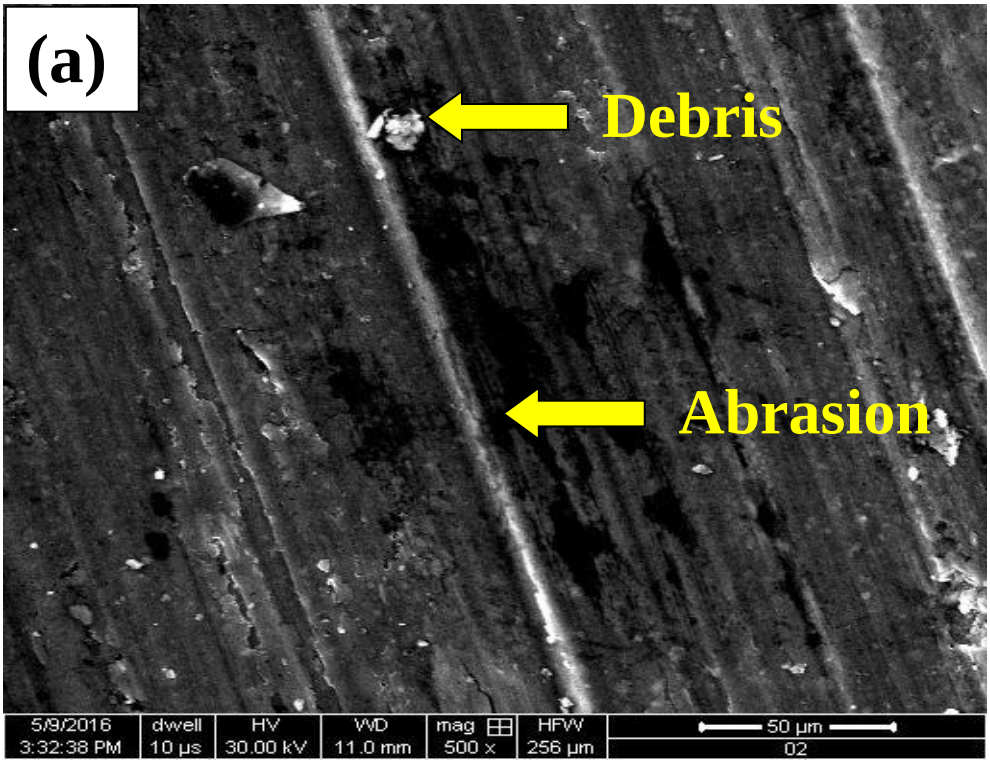

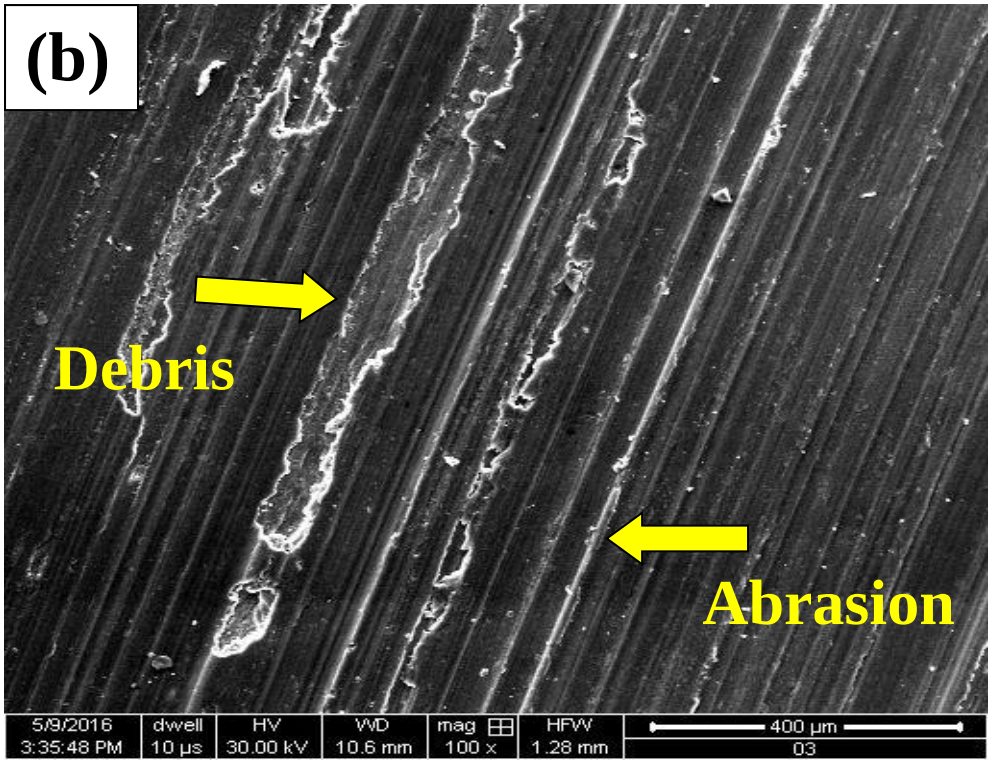

Figure 2.10:SEM micrographs of worn surfaces of a as cast after the first thermal cycle at different loads (a) 30N (b) 50N.

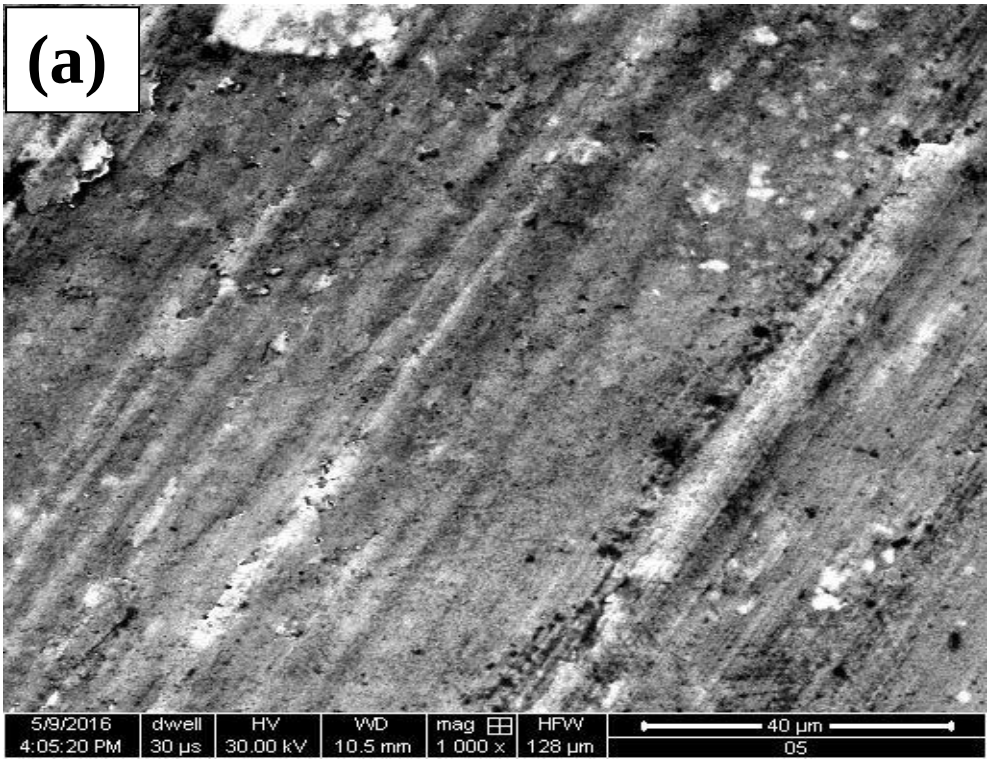

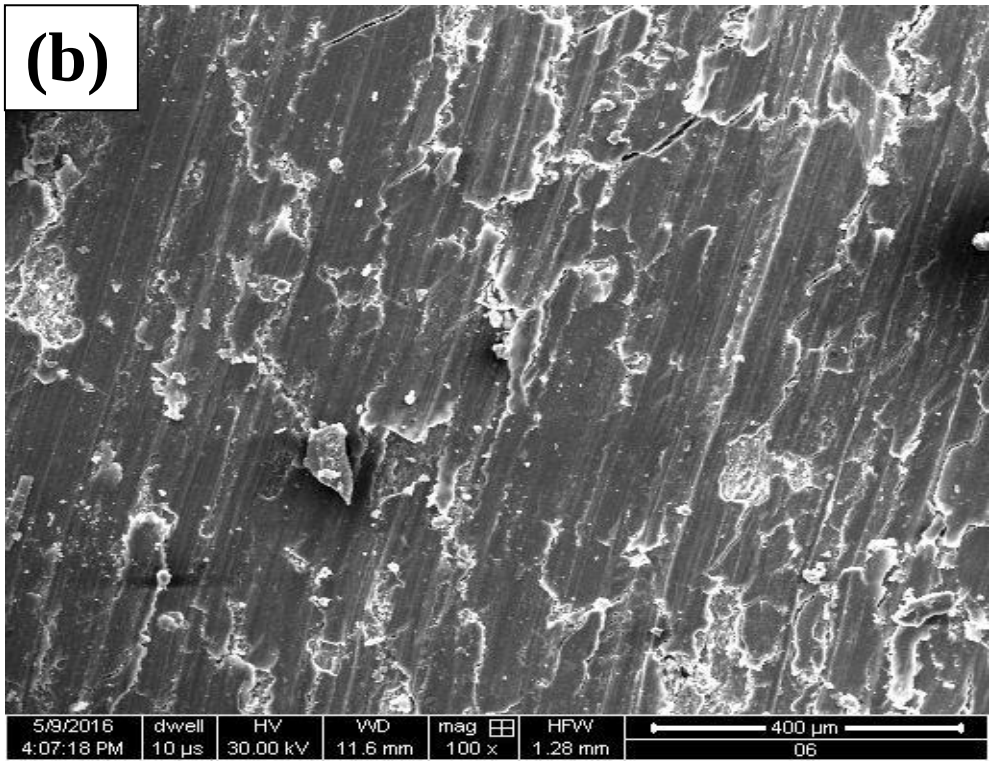

Figure 2.11: SEM micrographs of worn surfaces of a as cast after the fourth thermal cycle at different loads (a) 30N (b) 50N.

Fig. 2.12 shows the oxidative wear of 4th thermal cycled sample. Because of mixture of metallic and oxidative wear, the wear rate is less in 4th thermal cycled alloy compared to that of as cast and one single thermal cycled alloy. Jasim and Dwarkadasa(1982) and Suh(1980) worked on wear characteristics of Al-Si alloys against steel under dry sliding conditions. With increase in load, the wear changes from mild to severe transition and indicated oxidative wear mechanism at low load and metal cum oxidative wear was observed above the critical load [Jasim and Dwarkadasa, 1982 and Suh, 1980].

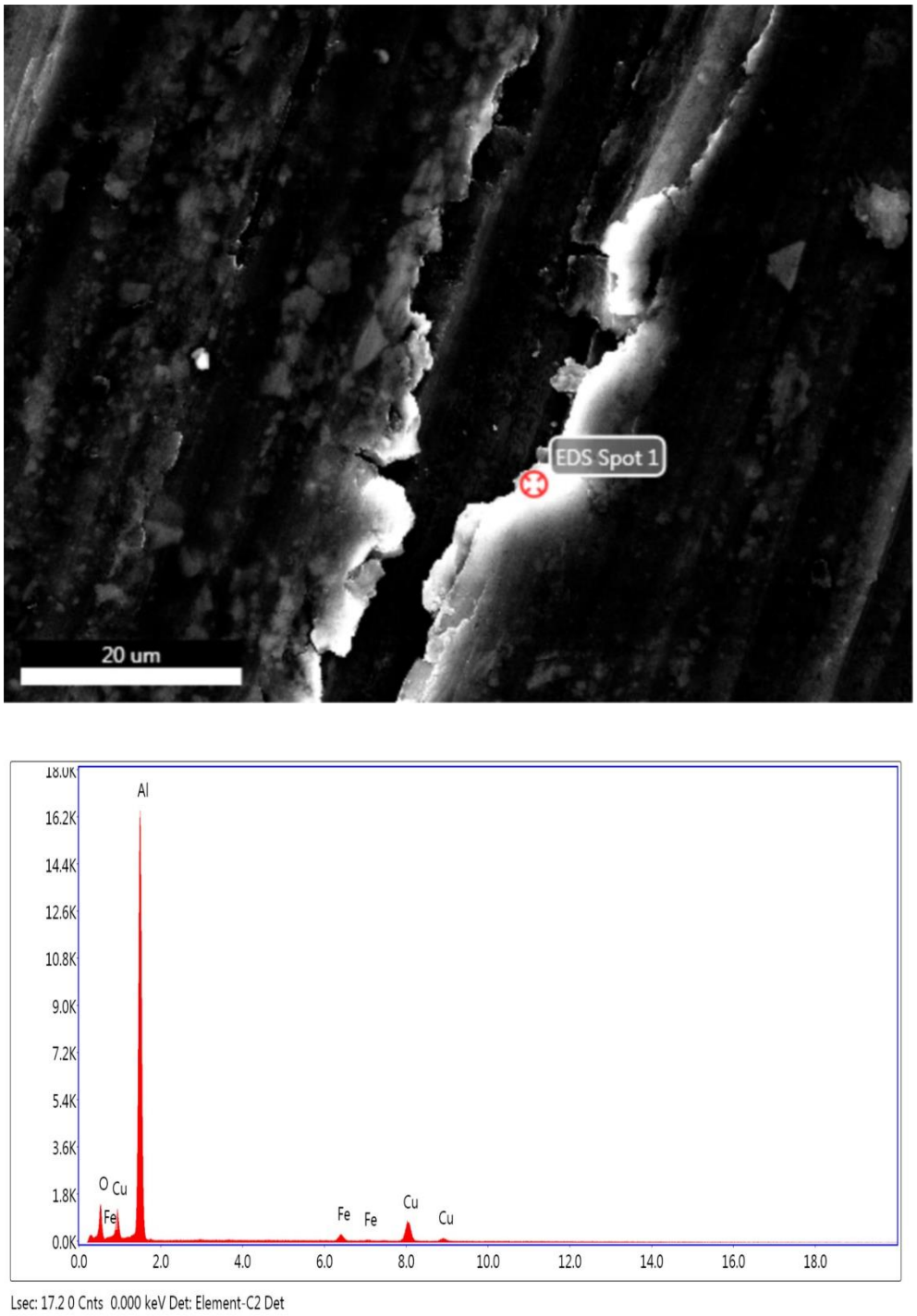

Figure 2.12: SEM micrographs and corresponding EDS of the wear track at1m/s sliding velocity and load of 50N.

2.4Conclusions

Thermal cycling of a hypoeutectic Al-10Cu alloy showed distribution of isolated droplets in the primary solid phase. The size of the droplets varied from 10 to 200μm arising from migration of liquid under temperature and concentration gradient. The inverse rate cooling curves indicated an undercooling of 20-35°C below the eutectic temperature of the alloy.

The solidification structure of droplets exhibited presence of fine particulate morphology of the eutectic phases in contrast to coarse lamellar eutectic microstructure in the inter-dendritic region of the as cast alloys. The decomposition of supersaturated solid solution phase resulting from large undercooling of droplets were explained for this anomalous behavior of the eutectic.

The wear property of the alloy was studied in a range of load varying from 20-50 N at sliding velocity 1.0 m/s. Distribution of droplets and their resultant solidification structure led to an improvement in the wear property of the alloy compared to the alloy processed by normal casting route. The nature of debris particles on wear surface provided information on low wear rate of the alloy into such Al-10Cu composite alloy configuration.